

Observation of Rabi oscillations between Bloch bands in an optical potential

M. C. Fischer, K. W. Madison, Qian Niu, and M. G. Raizen

Department of Physics, The University of Texas at Austin, Austin, Texas 78712-1081

(Received 8 June 1998)

We report an experimental study of atomic motion in the Bloch band of a periodic potential. Our system consists of cold sodium atoms in a far detuned standing wave of near resonant light. We prepare the atoms in the lowest motional band, and then impose phase modulation in order to drive interband transitions. We observe Rabi oscillations between the first and second band as a function of modulation intensity and frequency. We also observe damped oscillations of the population as a function of modulation frequency, which are primarily due to a spread in Rabi frequencies over the Bloch band. [S1050-2947(98)50110-2]

PACS number(s): 42.50.Vk, 32.80.Pj

The quantum behavior of particles in a periodic potential was analyzed by Bloch and Zener almost 70 years ago in order to understand electron conduction. They showed that stationary states of electrons in a lattice are plane waves modulated by periodic functions of position [1]. A wave packet that is initially localized in a potential well will spread via resonant ‘‘Bloch tunneling,’’ and will eventually become delocalized. The quantized energy levels are broadened into energy ‘‘bands’’ due to this tunneling process. The picture becomes considerably more complex when external fields (time varying or static) are imposed, and theoretical studies of such problems are still ongoing.

Quantum transport of particles in lattices has grown into an active area of research in recent years with the development of semiconductor superlattices. In a parallel development, the cooling of atoms to ultralow temperatures has opened up another field of study in which their center-of-mass motion exhibits manifestly quantum mechanical behavior, and experiments on quantum transport in optical lattices have probed a wide range of phenomena that are closely related to the condensed matter counterparts [2]. In this Rapid Communication, we report the observation of Rabi oscillations between Bloch bands of cold sodium atoms in the periodic potential of a standing wave of light [3]. This work relies on the long coherence times possible in atom optics, and opens up possibilities for coherent control of motional states in Bloch bands.

To begin our discussion we consider the effect of a standing wave of light on cold atoms. For sufficiently large detuning from resonance the effect of spontaneous emission can be neglected. Adiabatic elimination of the excited state leads to an effective one-dimensional potential of the form $V(x) = V_0 \cos(2k_L x)$, where $k_L = 2\pi/\lambda_L$ is the light wave number. The amplitude V_0 of the optical dipole potential is proportional to the laser intensity and inversely proportional to the detuning from resonance [4]. We add a time-dependent modulation of the standing wave position in the form

$$V(x,t) = V_0 \cos[2k_L x - \delta \cos(2\pi\nu t)], \quad (1)$$

where ν is the modulation frequency and δ is the dimensionless modulation amplitude. To elucidate the effect of this modulation we can expand the potential for small modulation amplitude δ . To first order, one obtains

$$V(x,t) = V_0 \cos(2k_L x) + V_0 \delta \sin(2k_L x) \cos(2\pi\nu t). \quad (2)$$

The first term in Eq. (2) is the stationary periodic potential that determines the eigenstates and eigenenergies of the system. The resulting set of quantized eigenenergies is periodic in momentum space and produces the well-known band structure. Figure 1 shows the energy bands in the reduced zone scheme within the first Brillouin zone. The graph corresponds to a typical well depth of $V_0/h = 70$ kHz, where h is Planck’s constant. When no perturbation of the potential is present, the quasimomentum q and the band index are conserved. The time-dependent second term in Eq. (2) has a small amplitude and can be treated perturbatively. It acts as a harmonic driving term that can induce transitions between the bands, leaving q unchanged. As indicated in Fig. 1 the drive frequency ν can be chosen to be resonant with the transition between the first two bands ($1 \leftrightarrow 2$), but far from resonance for transitions between successive bands [arrows (a) and (b)]. In this case only two eigenstates of the atoms need to be considered [5]. The population evolution in such a two-level system exhibits Rabi oscillations. If the drive frequency is close to resonance for both $1 \leftrightarrow 2$ and $2 \leftrightarrow 3$ [arrow

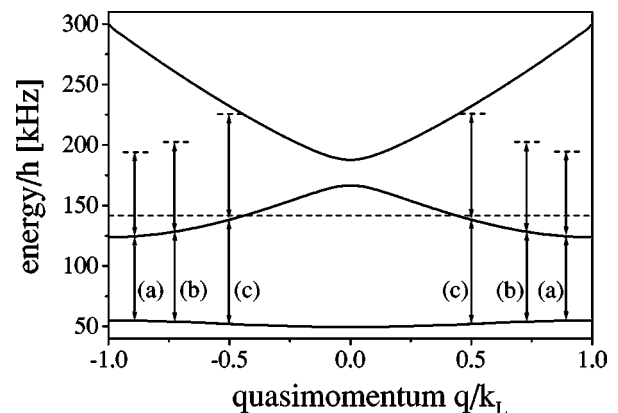


FIG. 1. Band structure for an atom in a far-detuned standing wave. The energies are calculated relative to the bottom of the potential for a well depth of $V_0/h = 70$ kHz. In the reduced zone scheme the quasimomentum q is limited to the first Brillouin zone $[-k_L, +k_L]$. The arrows correspond to a modulation frequency of (a) 70 kHz, (b) 75 kHz, and (c) 85 kHz. The dashed line indicates the top edge of the potential ($2V_0$).

(c) in Fig. 1] more than two levels participate in the interaction and more complicated dynamics are to be expected.

The experimental setup for measuring the transition between Bloch bands is based on the system previously used to study Wannier-Stark ladders and tunneling in optical lattices [6,7]. Several steps were necessary to prepare the atoms in the lowest Bloch band. We began by cooling and trapping a cloud of approximately 10^5 sodium atoms in a magneto-optical trap (MOT) in a $\sigma^+ - \sigma^-$ configuration [8]. The atom distribution in the MOT had a typical Gaussian width of $\sigma_x = (0.20 \pm 0.06)$ mm in position and $\sigma_p = (4.5 \pm 0.5) \hbar k_L$ in momentum. After the cooling and trapping sequence the magnetic field coils and the MOT beams were switched off and the interaction beam was turned on.

The interaction potential was a standing wave created by two linearly polarized counterpropagating laser beams with parallel polarization vectors. The light was far detuned from the $(3S_{1/2}, F=2) \leftrightarrow (3P_{3/2}, F=3)$ transition, and detunings typically ranged from 30 to 40 GHz. The power in each of the beams was adjusted up to 100 mW and was monitored with photodiodes during the interaction. The beams were spatially filtered to form a beam waist of 2.1 mm at the position of the atomic cloud. Due to the large momentum spread in the MOT, switching on the interaction potential initially populated several of the lower energy bands. As indicated in Fig. 1, the atoms projected into the lowest band are trapped within the potential wells, whereas atoms in the second band are only partially trapped. Atoms in even higher bands have energies well above the potential and, hence, are effectively free. To empty all but the lowest band, the standing wave was then accelerated to a velocity of $v_0 = 40 v_{\text{rec}}$, where $v_{\text{rec}} = 3$ cm/s is the single-photon recoil velocity. Linearly chirping the frequency of one of the counterpropagating beams, while keeping the frequency of the other beam fixed, resulted in a constant acceleration. As discussed in our previous work, accelerating the potential leads to a loss of population in the lower bands due to the tunneling of atoms into higher untrapped bands [7]. The transport acceleration a_{tr} was chosen to maximize tunneling out of the second band while minimizing losses from the first trapped band. For typical experimental parameters of $V_0/h = 70$ kHz and $a_{\text{tr}} = 2000$ m/s², the Landau-Zener expression for the lifetime of the first and second bands yields 24 ms and 40 μ s, respectively [9]. This ensured that, after 600 μ s of acceleration, only the first band still contained a significant number of atoms. After reaching the velocity v_0 the chirp was stopped and the frequency difference was held constant. At that point, phase modulation was added to one of the two counterpropagating beams forming the standing wave. The modulation was switched on and off smoothly over 16 μ s to avoid any discontinuous phase changes in the potential that could induce transition to higher bands. After a fixed time interval of zero acceleration the frequency chirping resumed at a rate corresponding to a_{tr} . This separated the remaining trapped atoms in the lowest band from those in higher bands in momentum space. After reaching a final velocity of 80 v_{rec} the interaction beams were switched off suddenly.

In the detection phase we needed to distinguish three classes of atoms: (1) atoms that were not initially trapped in the lowest band and immediately tunneled out of the well during the initial acceleration, (2) atoms that were trapped in

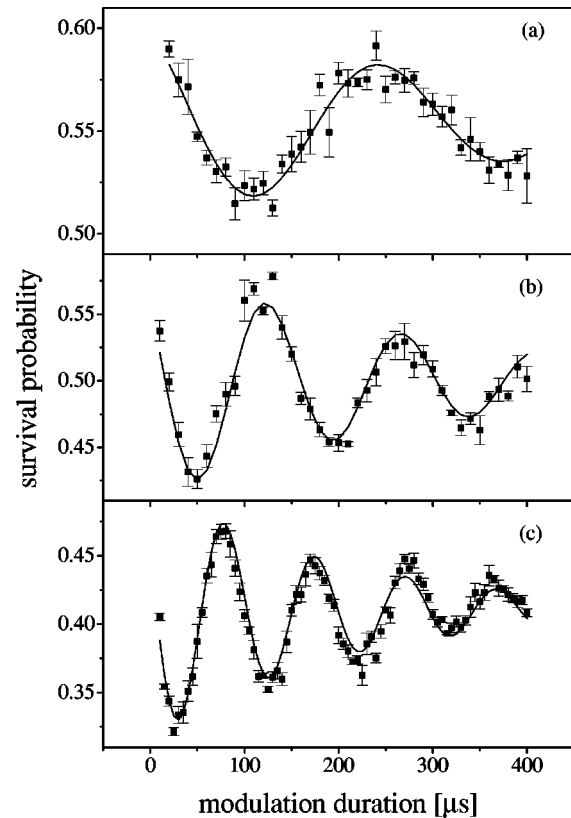


FIG. 2. Measured survival probability in the lowest band as a function of modulation duration. The modulation amplitude was set to be (a) $\delta=0.1$, (b) $\delta=0.2$, and (c) $\delta=0.3$. The data were taken at a well depth of $V_0/h=71$ kHz and a modulation frequency of $\nu=70$ kHz, corresponding to a drive near the band edge [as indicated in Fig. 1, arrow (a)]. Each run was repeated several times and the error bar denotes the one-sigma error of the mean. The solid line displays the fit of an exponentially damped cos function to the data.

the first band at the beginning of the interaction, but were driven out by the modulation, and (3) atoms that remained in the first band during the entire sequence. Since the atoms in different classes had left the trapping potential at a different stage of the experimental sequence, they were accelerated to different velocities. Therefore, after drifting in the dark for 2.5 ms, these classes separated in space and could be distinguished by recording their position. For this purpose the MOT beams were turned back on with no magnetic-field gradient present. This temporarily restricted movement of the atoms in a ‘‘freezing molasses’’ stage, while the fluorescence was imaged onto a charged coupled device camera. The two-dimensional image was then integrated in the direction that was perpendicular to the axis of the interaction beams to obtain a one-dimensional distribution along the beam direction, which contained all three classes of atoms. In order to reduce the sensitivity to fluctuations in the number of atoms in the MOT, the number of survivors [atoms in class (3)] was normalized by the total number of atoms initially trapped in the first band, which was obtained by summing up the contributions of classes (2) and (3). To observe the temporal evolution of the fundamental band population we repeated the experiment for various modulation durations, holding the modulation frequency ν and amplitude δ fixed.

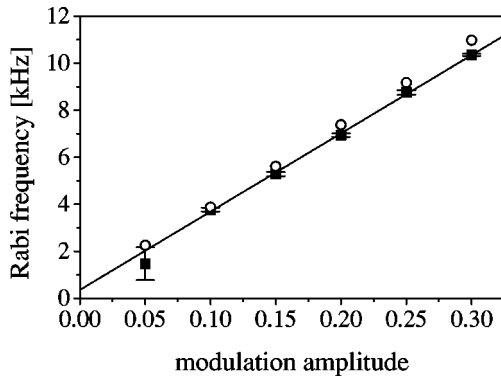


FIG. 3. The solid squares show the measured Rabi frequency versus the modulation amplitude for a well depth of $V_0/h = 71$ kHz and a drive frequency of $\nu = 70$ kHz. Uncertainties in the least-squares fit of the frequency are indicated as error bars. The line depicts the result of a linear least-squares fit through the experimental data. The hollow dots are the calculated Rabi frequencies for a drive at the band edge, corresponding to the experimental parameters.

Figure 2 compares the evolution of the first band survival probability for increasing modulation amplitude. The data were recorded for $V_0/h = 71$ kHz and $\nu = 70$ kHz, which corresponds to a drive resonant with states near the band edge as indicated by arrow (a) in Fig. 1. All graphs clearly show damped Rabi oscillations of the population in the first band. The damping can be explained by taking off-resonant transitions into account. Atoms with a quasimomentum close to the value for which the resonance occurs can undergo Rabi oscillations with different frequencies and different amplitudes [10]. Summing over the distribution of quasimomenta leads to a dephasing of the oscillations and, therefore, to a decrease in the average oscillation. It is important to note that this damping effect is not caused by level decay, since the Bloch states involved are stable. The plots of the survival probability in the first band in Fig. 2 show an overall offset from unity at zero modulation duration. We attribute this to the residual phase modulation of our standing wave, caused by incomplete extinction of the modulation signal, which drives transitions to higher bands. This introduces a constant loss independent of the chosen modulation duration and does not affect the curve shape. Because the strength of the residual modulation depends on the set modulation amplitude δ , the curve offset changes with increasing δ .

As is evident from Fig. 2, the frequency of the Rabi oscillation increases with the modulation amplitude. By fitting an exponentially damped cosine function to the experimental data, the value for the oscillation frequency can be extracted. The solid squares in Fig. 3 show the result of the least-squares fits. The error bars denote the uncertainty in the frequency fitting parameter. The plot in Fig. 3 shows a Rabi frequency that varies linearly with modulation amplitude δ . From the analytic solution of a driven two-level system one expects this linear relationship for the case of exact resonance. To compare this solution to the experimental data we calculated the Rabi oscillation frequency for a modulation driving transition only at the band edge. According to first-order perturbation theory, the expression for the resonant Rabi frequency is $\Omega = 1/h |\langle \Psi_1 | V_0 \delta \sin(2k_L x) | \Psi_2 \rangle|$, where $|\Psi_1\rangle, |\Psi_2\rangle$ are the unperturbed Bloch states in the first and

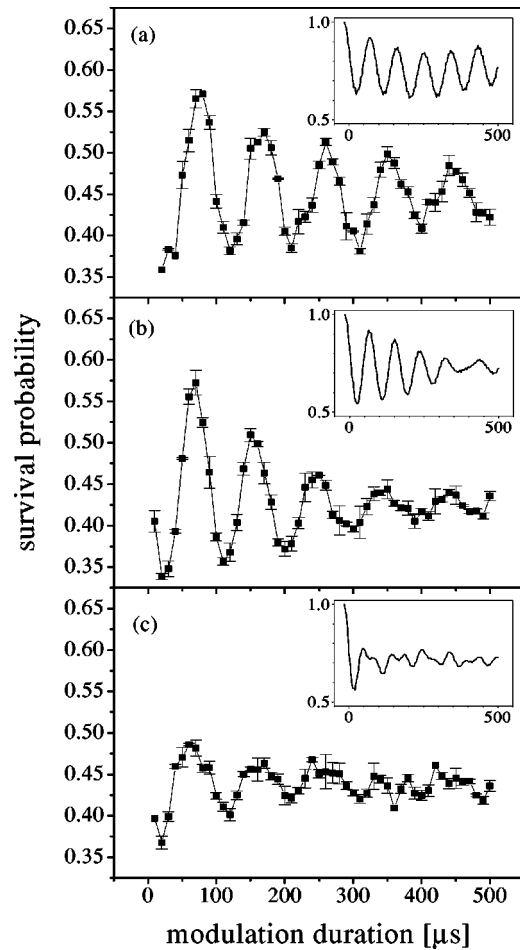


FIG. 4. Measured survival probability in the lowest band as a function of the modulation duration for three different frequencies. All of the data were recorded at a well depth of $V_0/h = 71$ kHz and a modulation amplitude of $\delta = 0.3$. The points are connected by solid lines for clarity. The insets show the results of numerical simulations at $V_0/h = 72$ kHz and $\delta = 0.3$. Note that the modulation duration does not include the 16- μ s turn-on and turn-off times. The modulation frequency was set to be (a) $\nu = 70$ kHz, (b) $\nu = 75$ kHz, and (c) $\nu = 85$ kHz, corresponding to drives that are indicated by the arrows in Fig. 1.

second bands respectively. The resulting frequencies are displayed as hollow dots in Fig. 3, in which a slight detuning of the drive from the transition $1 \leftrightarrow 2$ has been taken into account. The calculation results are in good overall agreement with the experimental data. The slight deviation in frequency of the measured versus the calculated data can be attributed to the experimental uncertainty in the determination of the well depth V_0 . We can measure the intensity of the interaction beams to within $\pm 10\%$, which leads to the same relative error in the value for the well depth. To check the validity of restricting the range of quasimomenta to the band edge, we performed a numerical integration of Schrödinger's equation, including the full potential in Eq. (1), with an initial condition that was taken to be a uniform distribution of atoms in the first band. The frequencies of the resulting population oscillations are not plotted in Fig. 3 because, on the scale used, they are indistinguishable from the calculated values. The calculation and the numerical integrations were performed using experimental values, for the well depth and

drive frequency, with no adjustable parameters.

Driving transitions at the band edge has several advantages, one of which is the high density of states in that region. This results in a large number of atoms that can participate in the population transfer, therefore yielding a large detection signal. Another advantage is the slow damping rate of the Rabi oscillations. Since there is a large fraction of atoms contributing to the oscillation with the same frequency, the small number of off-resonantly driven atoms will not significantly decrease the amplitude of the averaged oscillation. Away from the band edge, however, the relative weight of the resonant oscillation frequency becomes less dominant and the off-resonant drives lead to an increased damping rate. The evolution of the first band population for three different drive frequencies is depicted in Fig. 4. The data were recorded at a well depth of $V_0/h=71$ kHz and a modulation amplitude of $\delta=0.3$. The insets show the result of the numerical integrations, for which the well depth was adjusted to $V_0/h=72$ kHz in order to produce matching damping rates. The modulation frequencies in Figs. 4(a)

through 4(c) match the corresponding arrows in Fig. 1 [(a) 70 kHz, (b) 75 kHz, and (c) 85 kHz]. Larger damping rates for increasing modulation frequencies are clearly visible. In addition, we observed a decrease in oscillation amplitudes due to a smaller density of states at the center of the band. At the opposite side of the energy band lower damping rates are recovered. Modulating the potential with frequencies beyond the band edges leads to Rabi oscillations with a higher frequency and a lower amplitude, as expected for off-resonantly driven systems (not shown).

In summary, we have observed Rabi oscillations of atomic population between Bloch bands in an optical potential. Future directions include spectroscopic studies of the band structure modified by external fields, and the preparation of novel motional states in Bloch bands.

We thank Roberto Diener for help with the calculations and numerical simulations. This work was supported by the Robert A. Welch Foundation and the National Science Foundation.

-
- [1] F. Bloch, *Z. Phys.* **52**, 555 (1929); C. Zener, *Proc. R. Soc. London, Ser. A* **145**, 523 (1934).
- [2] M. G. Raizen, C. Salomon, and Q. Niu, *Phys. Today* **50** (7), 30 (1997).
- [3] X.-G. Zhao, G. A. Georgakis, and Q. Niu, *Phys. Rev. B* **54**, R5235 (1996).
- [4] R. Graham, M. Schlautmann, and P. Zoller, *Phys. Rev. A* **45**, R19 (1992).
- [5] Assuming that all the atoms are initially in the first band, the resonant coupling for arrow (a) between the second and third bands for a different quasimomentum can be neglected, since those states are not populated.
- [6] S. R. Wilkinson, C. F. Bharucha, K. W. Madison, Q. Niu, and M. G. Raizen, *Phys. Rev. Lett.* **76**, 4512 (1996).
- [7] C. F. Bharucha, K. W. Madison, P. R. Morrow, S. R. Wilkinson, B. Sundaram, and M. G. Raizen, *Phys. Rev. A* **55**, R857 (1997); S. R. Wilkinson, C. F. Bharucha, M. C. Fischer, K. W. Madison, P. R. Morrow, Q. Niu, B. Sundaram, and M. G. Raizen, *Nature (London)* **387**, 575 (1997).
- [8] For a recent review, see S. Chu, *Science* **253**, 861 (1991).
- [9] Q. Niu, X.-G. Zhao, G. A. Georgakis, and M. G. Raizen, *Phys. Rev. Lett.* **76**, 4504 (1996).
- [10] The Rabi frequency also depends on the transition matrix element for the given quasimomentum. However, for the transition $1 \leftrightarrow 2$, the matrix elements are constant within about 10%.